

Field dependence of the magnetization of granular Y-Ba-Cu-O

U. Yaron, Y. Korniyushin, and I. Felner

Racah Institute of Physics, The Hebrew University, Jerusalem, Israel

(Received 27 March 1992; revised manuscript received 16 July 1992)

We have studied the field dependence of the zero-field-cooled magnetization of granular Y-Ba-Cu-O samples of different packing factors (between 10% and 80%). We discuss the competition between the demagnetizing factors of the sample, N , and that of the grains, n . Applying the Clausius-Mossotti approximation, we suggest a phenomenological model to treat the experimental results. According to the model the effective demagnetizing factors N_{eff} depend on the fraction of shielded volume, which is itself a field-dependent quantity. At low fields, N_{eff} approach N and n for highly compact and dilute samples, respectively. The suggested analysis enables the distinction and characterization of the different contributions to the total volume of the sample.

I. INTRODUCTION

Much of our information regarding high- T_c superconductors has been obtained through magnetization measurements of granular ceramics. The magnetization values and the parameters extracted from them could be extremely difficult to handle, since the detailed magnetic structure of inhomogeneous samples is not perfectly clear. The magnetization of sintered samples is governed by the effective demagnetization field seen by the sample. The calculation of this field could be extremely difficult, as the shape of the whole sample is generally and usually not an ellipsoid and as there is a competition between the demagnetizing factors of the macroscopic sample on the one hand and that of the grains on the other.

For cylinders the calculation of the demagnetizing factors is not straightforward, since the magnetization is not homogeneous and in general, varies throughout the cylinder in both the radial and axial direction. This problem has been theoretically addressed by Chen, Brug, and Goldfarb¹ who have calculated the demagnetizing factors for cylinders as a function of the susceptibility and the aspect ratio, assuming that the cylinder is homogeneous and consists of material with constant susceptibility. Their results are consistent with an earlier work of Taylor,² which predicts that for a diamagnetic cylinder ($\chi < 0$), the sum of the demagnetizing factors along the principal axes of the cylinder, should be larger than 1. The demagnetizing factors of cylinders have been extracted experimentally by Kunchur and Poon³ from magnetization measurements on lead and Nb-Ti discs. They found that the ellipsoidal approximation is not suitable for cylinders with large aspect ratios.

The competition between the demagnetizing factors of the whole sample and of the grains has been investigated by Senoussi *et al.*,⁴ who have performed magnetic measurements on sintered Y-Ba-Cu-O pellets and on oriented grains dispersed in epoxy resin. They have shown that for highly compact specimens with packing factors $> 85\%$ the demagnetizing factors are imposed by the macroscopic shape of the sample, and these for low-

density samples are governed by the geometrical shape of the individual grains. This result is consistent with calculations made by Maxwell and presented in his Treatise,⁵ from which one can conclude that for a dense mixture the effective demagnetizing factors are that of the pellet, not the grains, even when the grains are decoupled by external field.

A further complication of the description of the magnetization of inhomogeneous granular ceramic superconductors is the field dependence of the shielded volume, which contributes to the diamagnetic signal. An increase of the applied field H_0 causes an increase of the amount of flux penetrating the weak links and grains and thus leads to a monotonic decrease of the volume that is shielded from the magnetic induction, B . This decrease is expressed in $M(H_0)$ curves by an increasing deviation from linearity, even below H_{c1} of the grains. The non-linear field dependence of the moment of ceramics is different from that observed in single crystals,⁶ for which M is quite linear even in fields exceeding H_{c1} . It seems that although some effort has been made, a detailed study of the magnetization as a function of H_0 of granular ceramic superconductors is nevertheless needed.

In order to clarify and to elucidate this problem we have carried out a detailed study of polycrystalline Y-Ba-Cu-O cylinders of different dimensions in a large range of packing factors, between 10 and 80%. The samples were zero-field cooled down to 4.2 K and the magnetic moments were measured as a function of applied field H_0 up to 1000 Oe, in two perpendicular orientations [\mathbf{H}_0 parallel to the axis of the cylinder, c ($\mathbf{H}_0 \parallel c$), and parallel to the radius of the cylinder, r ($\mathbf{H}_0 \parallel r$)]. Typical M vs H_0 curves in both directions, that of sample 3, are presented in Fig. 1(a). The ratio of the magnetic moments, $M_c/M_r \approx 1.35$ is almost constant in the whole field range. This ratio is smaller than ≈ 1.6 , one would expect by approximating the cylinder to be an ellipsoid of revolution, and using demagnetizing factors from conventional tables.⁷ This inconsistency is quite obvious, since our sample is *not homogeneous* and the macroscopic dimensions of the sample are not the only relevant dimen-

sions. Furthermore, Taylor's calculations for *homogeneous* cylinder predict that its anisotropy ratio should be smaller than that of an ellipsoid with the same aspect ratio.² Since the ratio M_c/M_r is field independent one can naively replace the applied field by an effective internal field $H_{\text{eff}}=H_0/(1-N_e)$ using effective demagnetizing factors N_e , which are field independent, and scale the two curves of Fig. 1(a) into one curve [see Fig. 1(b)]. The extent of the scaling is good throughout the whole field range, and is not altered at fields exceeding H_{c1} . In fact, this method could serve as an experimental tool to extract N_e of polycrystalline samples. However, as we show below, this treatment of the experimental results, simple and straightforward as it is, is not justified. In this paper we show that the effective demagnetization factors depend on the fraction of the shielded volume f , which is itself a field-dependent quantity, and thus the scaling has a different origin.

Spatial distribution of the magnetic field in a superconductive (SC) sample determines in great extent its magnetic properties. To evaluate these properties, one has to clear up the picture of the physical state of inhomogeneous sample and use a system of conceptions that allows

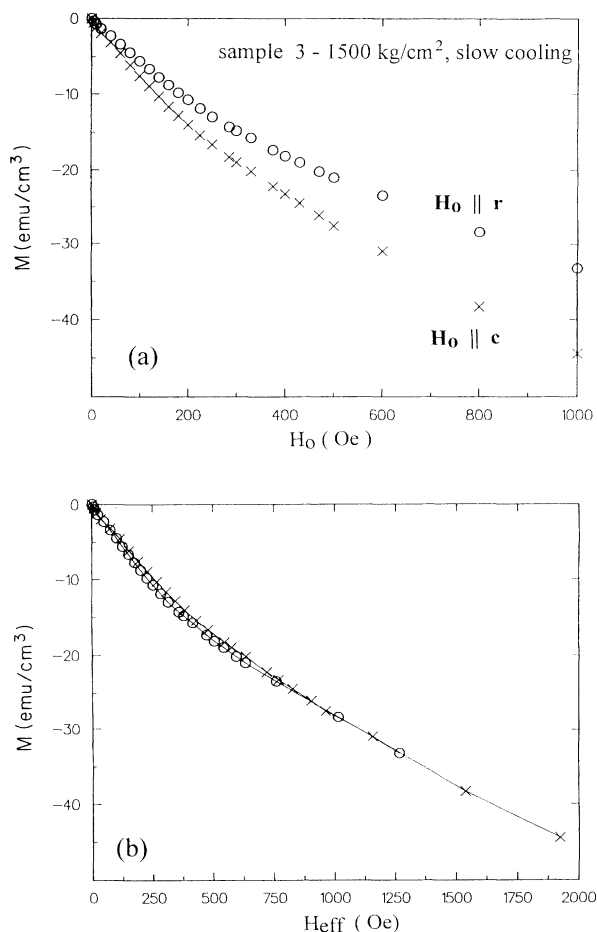


FIG. 1. (a) Applied field dependence of M of sample 3 for $H_0 \parallel c$ and $H_0 \parallel r$. (b) The same data drawn as a function of $H_{\text{eff}} = H_0/(1 - N_e)$.

one to perform calculations. The exact calculation of the distribution of the field and the magnetic moment in a sample is a problem of extreme mathematical difficulty. To approach the solution of the problem one has to use a model notion. Field flow through a ceramic SC pellet was considered previously by Reich and Nabutovsky,⁸ who estimated the strength of the weak SC links in a granular system. They claim applicability of their model and experimental results to the case of a small shielded fraction. Holdron, Navarro, and Campbell,⁹ systematically investigated the dependence of the field value in the intergranular area for small H_0 . They considered SC spheres, immersed in a magnetic field, which is homogeneous far away from the spheres. Their results refer mainly to cylinders with its long axes parallel to H_0 . In Sec. II, we propose a simple phenomenological model, which connects the measured magnetic moment of the SC granular sample and H_0 , even at high H_0 , for different orientations of dilute and dense materials. This model is used as a basis for the treatment of the experimental results that follow.

II. THEORETICAL MODEL

The model assumes that flux lines penetrate through the granular ceramics along the nonsuperconductive areas, percolating the sample, while the rest of the sample remains shielded. This implies a certain magnetic structure of the sample. As the conditions of the problem fairly correspond to the framework of the linear electrodynamics, the measured density of the magnetic moment M should depend linearly on H_0 , only when the magnetic structure of the sample is independent on H_0 . So, non-linear dependence of M on H_0 is a consequence of the changes in the magnetic structure of the sample with increasing H_0 . On the other hand, the magnetic structure of a given sample is determined by the value of the magnetic field inside the percolating nonsuperconductive areas (PNA), which in the general case depends on the orientation of the sample with respect to H_0 . Hence, for a definite, fixed value of H_0 , we may have different magnetic structures of the same sample, depending on its orientation. From this it follows that the well-known relationship between the components of the demagnetizing factors (namely that their sum is equal to 1) does not necessarily hold. In a case of inhomogeneous sample (such as granular ceramic sample) the values of magnetic field inside the sample are inhomogeneous as well. By increasing the external field, we may reach a critical value of a field in some parts of the sample, changing in this way its magnetic structure. All this manifests itself in the values of magnetic moment and the calculated shielded fraction of the sample.

To describe the shielded state of the granular superconductor, we have to formulate a model that takes into account (a) the shape of the sample, (b) the shape of the shielded volume elements (SVE), (c) the penetration of flux through the PNA, and (d) the flux density in the SVE when the field in them, H_s , exceeds H_{c1} . In the theory of mesoscopically inhomogeneous samples there are two simple approaches: The Clausius-Mossotti (CM) approxi-

mation, commonly used in dielectric theory,¹⁰ and the effective-medium theory of Bruggeman.¹¹ Both approaches are thoroughly reviewed by Landauer.¹² The CM approximation is applicable to more or less regular structures, while the effective-medium theory takes into account random distribution of inhomogeneities. In ceramic materials the grains do not overlap and are, in general, separated by intergranular weak links and pores, so we consider the concept of CM as more appropriate. The model to be described next, corresponds to this approximation applied to our specific case.

Model: Due to the influence of the shape of the sample, the connection between the internal field H_i and H_0 is given by

$$H_i = H_0 - 4\pi NM, \quad (1)$$

where H_i and M are the internal field and magnetic moment averaged over the entire volume and N is the macroscopic demagnetizing factor. It is supposed, as well, that $M=0$ inside the PNA (including percolating pores) and that the boundaries between the SVE and PNA are sharp. We further introduce the effective homogeneous magnetic field inside the PNA, H , which plays the role of the external field with respect to the SVE. Hence the average value of the magnetic field inside the SVE, H_s , could be described as

$$H_s = H - 4\pi n M_s, \quad (2)$$

where n is the demagnetizing factor and M_s is the specific (per unit volume) value of the magnetic moment of the SVE. If V is the volume of the sample, and v is the shielded volume, the shielded fraction is given by $f = v/V$ and

$$H_i = (1-f)H + fH_s = H - 4\pi n f M_s = H - 4\pi n M, \quad (3)$$

where Eq. (2) is used, as is the fact that $M = fM_s$, since $M=0$ inside the PNA. Comparing Eqs. (1) and (3) we get

$$H = H_0 - 4\pi M(N - n); \quad (4)$$

inserting Eqs. (3) and (4) into Eq. (2) we get

$$H_s = H_0 - 4\pi [fN + (1-f)n]M/f. \quad (5)$$

The induction B inside the SVE is given by

$$B_s = H_s + 4\pi M_s = H_0 + 4\pi [1 - fN - (1-f)n]M/f, \quad (6)$$

and after rewriting this we obtain

$$M = -\frac{H_0 - B_s}{4\pi} \frac{f}{1 - fN - (1-f)n}. \quad (7)$$

This equation could be rewritten once more in a way that emphasizes the physics behind it:

$$M = -\frac{H_0 - B_s}{4\pi} \frac{f}{1 - N_{\text{eff}}}, \quad (8)$$

where

$$N_{\text{eff}} = fN + (1-f)n. \quad (9)$$

N_{eff} are the effective demagnetizing factors. This terminology is based on the comparison of Eq. (8) to a similar equation describing the field dependence of the magnetic moment of single crystals.⁶ According to Eq. (9), N_{eff} is a weighted average of the demagnetizing factors of the SVE and of the sample as a whole. In a case of $f=1$ we have $N_{\text{eff}}=N$, while for $f \ll 1$ we obtain $N_{\text{eff}} \approx n$. This result implies that for highly compact samples in low fields, the effective demagnetizing factors are imposed by the macroscopic shape of the sample, and for samples with low packing factors they are governed by the shape of the individual shielded elements, as shown experimentally by Senoussi *et al.*⁴

Let us consider separately the case of complete shielding of the SVE ($B_s=0$). In this case we get from Eqs. (2), (4), (7), and (9) that

$$H = H_0(1-n)/(1-N_{\text{eff}}) \quad \text{and} \quad H_s = H_0/(1-N_{\text{eff}}). \quad (10)$$

Rewriting Eq. (7) we get, in this case,

$$f = \frac{(1-n)M}{M(N-n) - H_0/4\pi}, \quad (11)$$

a formula that will later serve in the analysis of the experimental data.

III. EXPERIMENTAL DETAILS

The experimental study has been performed on polycrystalline Y-Ba-Cu-O cylinders (diameter, 0.5 cm) of different packing factors and thicknesses. The Y-Ba-Cu-O material was prepared by conventional solid-state reaction. The appropriate amount of the oxides was pressed into pellets and heated to 950°C for 24 h and then ground into powder. This procedure was repeated twice. In order to obtain the highly packed samples (77% samples 1, 2, 5, and 6) the powder was pressed at 9200 kg/cm². The samples with packing factor 65% (3 and 4) were obtained by pressing the powder at 1500 kg/cm². With the intention to control the sizes of the grains and the strength and nature of the weak links the samples (samples 1–6) were treated by different heat treatments, which followed a 2 h sintering at 950°C. Samples 1, 3, 5, and 6 were cooled to 450°C at a slow rate of 10°C/h, while samples 2 and 4 were furnace cooled in this interval of temperatures ($\approx 100^\circ\text{C/h}$ during the first hour). All samples were further annealed at 450°C and furnace cooled to room temperature under flow of oxygen. The lower-density samples (30% and 10%, samples 7 and 8, respectively) were obtained by mixing annealed Y-Ba-Cu-O powder with methyl methacrylate polymer. The parameters related to all samples are summarized in Table I. All samples were characterized by scanning electron microscopy (SEM), which enabled the determination of the typical sizes of grains (between 2 and 10 μm , for sample 4 and 1, respectively) and the estimation of the contribution of intergranular material and pores to the total volume.

Magnetic measurements reported here were carried on a commercial PAR 155 vibrating sample magnetometer, which enables a rotation of the sample relative to the

TABLE I. Packing factors, dimensions, and preparation methods of the Y-Ba-Cu-O cylinders used in the experimental study. The details are described in the text.

Sample No.	Packing factor	Diameter (cm)	Thickness (cm)	Pressure (kg/cm ²)	Cooling rate	Remarks
1	77%	0.5	0.25	9200	10°C/h	
2	77%	0.5	0.25	9200	fast	
3	65%	0.5	0.25	1500	10°C/h	
4	65%	0.5	0.25	1500	fast	
5	77%	0.5	0.20	9200	10°C/h	
6	77%	0.5	0.30	9200	10°C/h	
7	30%	0.5	0.25			polymer
8	10%	0.5	0.25			polymer

external field direction. All samples were cooled to 4.2 K under nominal zero field (less than 1 Oe), at different orientations. A field was subsequently applied and the magnetic moment was recorded as a function of the applied field, H_0 . All measurements described here were performed at 4.2 K.

IV. EXPERIMENTAL RESULTS AND DISCUSSION

The volume of a granular sample could be described as the sum of four contributions: (a) the volume of grains, (b) the volume of weak links, (c) the volume of the nonsuperconducting intergranular material, and (d) the volume of shielded (surrounded by superconductive material) and unshielded pores. At high fields the SVE are composed only of grains, and the effective field inside the grains, H_g , could replace H_s , while at lower fields the weak links and the shielded pores are parts of the SVE as well.

The applied field dependence of M for ceramic samples is described by Eq. (8). The nonlinearity (Fig. 1) is a consequence of a decrease of the shielded volume f and penetration of flux into it, leading to an increase of B_s , as the applied field is increased. As long as $H_g < H_{c1}^{\text{grains}}$ the nonlinearity is governed by a decrease of f , caused mainly by the transition of the weak links from superconductive (field in the weak links smaller than H_{c1}^{wl}) to the normal state (field in the weak links larger than H_{c2}^{wl}). The grains in this interval remain shielded (except for the London penetration shell, which is by definition unshielded), while the weak links are either totally shielded ($H_s < H_{c1}^{\text{wl}}$), partially shielded ($H_{c1}^{\text{wl}} < H_s < H_{c2}^{\text{wl}}$) or not being part of the SVE (weak links in the normal state). It is therefore that as long as H_g is smaller than H_{c1}^{grains} , B_s , which is the average of B over the entire volume of the SVE, is either zero or negligible. We thus apply Eq. (11) to this field regime.

A. Demagnetizing factors

Equation (11) contains two unknown quantities, namely N and n , which are the demagnetizing factors of the macroscopic sample and the grains, respectively. The SVE of samples 1–8 could be assumed spherical and thus $n = 1/3$. In order to evaluate N , M vs H measurements at 4.2 K were performed on lead metal cylinders of dimensions similar to those of the Y-Ba-Cu-O samples

given in Table I. The measurements were performed on both $\mathbf{H}_0 \parallel \mathbf{c}$ and $\mathbf{H}_0 \parallel \mathbf{r}$. N_r and N_c , which were extracted from the different slopes of M vs H curves in the $H_0 < H_c(1-N)$ regime are similar to those calculated approximating the cylinders to be ellipsoids with the same aspect ratio. This result is consistent with previously published results,³ which found an essential disagreement between the two, only for lead cylinders with much higher aspect ratios. For the lead cylinder with dimensions identical to samples 1–4, 7, and 8, we extract $N_c = 0.53(1)$ and $N_r = 0.23(2)$. The sum $N_c + 2N_r = 0.99(5)$ is smaller than 1.114 calculated by Taylor² for a superconducting cylinder with the same aspect ratio. It should be noted that the demagnetizing factors could be also received by dividing the location of the deviation of M from linearity at $H_0 = H_c(1-N)$ by H_c . This approach leads to somewhat different demagnetizing factors, a fact which was previously discussed.⁵

B. Results related to the compact samples (1–6)

We measured the applied field dependence of the magnetic moment at 4.2 K of samples 1–6 in both $\mathbf{H}_0 \parallel \mathbf{c}$ and $\mathbf{H}_0 \parallel \mathbf{r}$ directions. Generally speaking, the field dependence of M for all samples in both directions are quite similar and typical curves, that of sample 3, are exhibited in Fig. 1. As mentioned above, the shape of the curves is described by Eq. (8). The $M(H_0)$ dependence is qualitatively different than that observed on single crystals.⁶ The single-crystals curves are quite linear even in fields exceeding H_{c1} , whereas the deviation from linearity observed in polycrystalline samples is much more pronounced. This difference could be readily explained on the basis of critical state models.^{13,14} The relevant dimensions for applying these models to ceramic samples in fields exceeding H_{c2}^{wl} (wl—weak links) are the dimensions of the grain, while for single crystals they are the external dimensions of the crystal. The field gradient inside the superconducting material is independent of dimensions, and thus the field profile inside a single crystal differs from that of an ensemble of grains with similar volume.

Figures 2(a) and 2(b) show the shielded fraction f of samples 1–4 for $\mathbf{H}_0 \parallel \mathbf{c}$ as a function of H_0 , calculated using Eq. (11), with $n = 1/3$ and $N_c = 0.53$. One can immediately recognize the four different regimes in the curves.

(a) $H_s < H_{c1}^{wl}$ —The shielded fraction f of samples 1 and 3 (the samples that were cooled slowly after sintering) is constant. From Fig. 2(b), using Eq. (10) to determine H_s from H_0 , we extract $H_{c1}^{wl} \approx 10$ Oe. For samples 2 and 4, which were obtained by cooling at a much faster rate, which does not allow the formation of weak links with homogeneous characteristics, the behavior is different. For these samples we do not find an interval of constant shielded fraction and a well defined H_{c1}^{wl} . Note also, that f of samples 1 and 3 is smaller than that of samples 2 and 4. We interpret this result on the basis of difference in the concentration of shielded pores in the samples. Long heat treatments lead to coalescence of closed shielded pores to a larger, open and unshielded pore, and thus cause a lowering of the shielded fraction in this regime.

(b) $H_{c1}^{wl} \leq H_s \leq H_{c2}^{wl}$ —This interval is characterized by a sharp decrease of f . The location of H_{c2}^{wl} is quite well defined for all samples [Fig. 2(b)], and using Eq. (10), we extract $H_{c2}^{wl} \approx 50$ Oe.

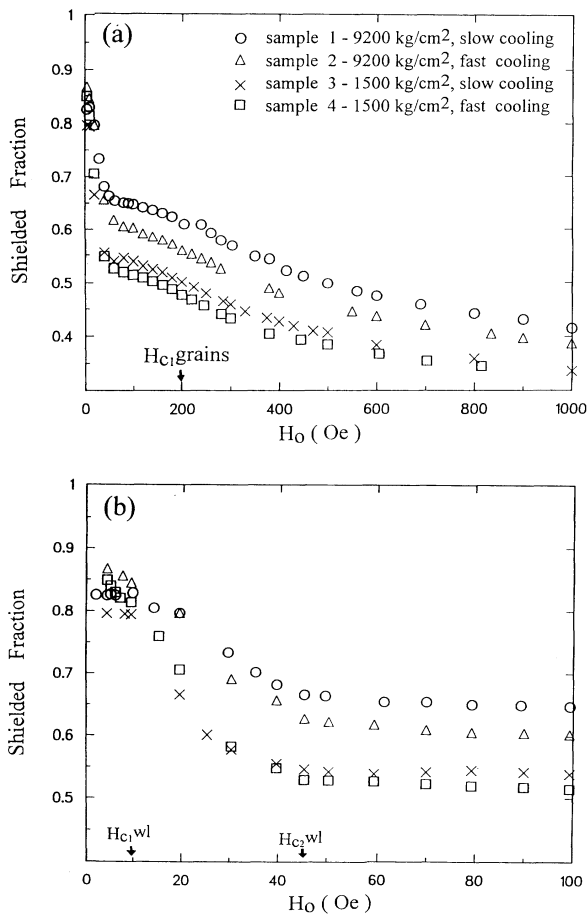


FIG. 2. The applied field dependence of the shielded fraction f of samples 1–4 for $H_0 \parallel c$, calculated using Eq. (11), for (a) $H_0 < 1000$ Oe and (b) $H_0 < 100$ Oe. The decrease of f for $H_g > H_{c1}^{grains}$ is less pronounced than that presented in this figure, since the assumption that $B_s = 0$ is not justified in this field interval.

(c) $H_{c2}^{wl} \leq H_s$; $H_g \leq H_{c1}^{grains}$ —The shielded fraction is nearly constant. The location of H_{c1}^{grains} is smeared due to inhomogeneous grains' characteristics. In this field regime the shielded fraction hierarchy is such that

$$f_{1500,fast} < f_{1500,slow} < f_{9200,fast} < f_{9200,slow}, \quad (12)$$

where the subscripts are related to the pressure applied to the powder during pressing and to the cooling rate. This reasonable result means that large pressing force and slow cooling rates increase the fraction of the grains in the total volume of the sample and their typical size. The effect of the grain size on f is introduced by the ratio λ/r_g of the London penetration depth to the grain size, controlling the contribution of the nonshielded London penetration shell to the total volume of the grain. SEM studies of the samples show similar hierarchy in the typical sizes of the grains (between $2 \mu\text{m}$ and $10 \mu\text{m}$).

(d) $H_g \geq H_{c1}^{grains}$ —characterized by a continuing decrease of the shielded fraction. It should be noted that for fields higher than H_{c1}^{grains} the treatment of the data with Eq. (11) is not justified, since the contribution of B_s to M [Eqs. (7) and (8)] could not be neglected anymore. It is therefore that the decrease of the actual shielded fraction in this interval is less pronounced than that presented in Fig. 2(a).

The obtained H_{c1}^{wl} and H_{c2}^{wl} values are consistent with values published by Senoussi *et al.*⁴ The sharp drop in f in the range $H_{c1}^{wl} \leq H_s \leq H_{c2}^{wl}$ [Fig. 2(b)] may serve as a tool to estimate the volume of the weak links and the pores surrounded by superconductive material, which is between 15% (sample 1) and 35% (sample 4) of the total volume of the sample. The field dependence of f for $H_0 \parallel c$ of samples 5 and 6, which differ from sample 1 only by their external dimensions, is very similar to that of sample 1.

According to Eq. (9), the effective demagnetizing factor depends on f . For these samples $N_r < n < N_c$, and thus the weighted averaging suggested by this equation leads to an increase of N_{eff}^r and a decrease of N_{eff}^c (Fig. 3) as f

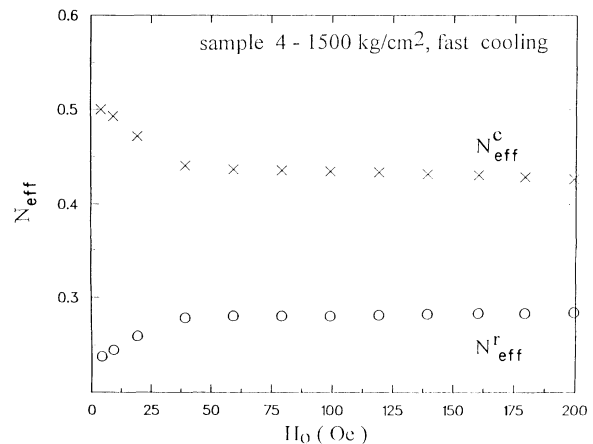


FIG. 3. The applied field dependence of N_{eff}^c and N_{eff}^r of sample 4. Note that at low fields they approach N_c and N_r , respectively.

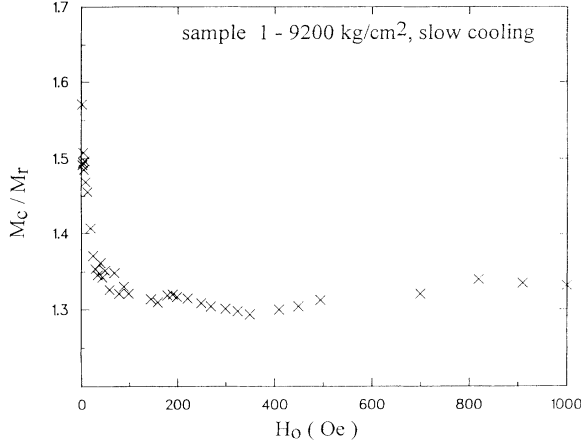


FIG. 4. The applied field dependence of M_c/M_r of sample 1. Note that at low fields the ratio approaches $(1-N_r)/(1-N_c) \approx 1.6$, and that at fields exceeding H_{c2}^{wl} it is essentially constant.

decreases. In the low-field limit, f is quite high and N_{eff}^c and N_{eff}^r approach the demagnetizing factors of the sample as a whole ($N_c = 0.53$ and $N_r = 0.23$). As mentioned above, these values are similar to that received by approximating the cylinder by an ellipsoid with the same aspect ratio.

For $\mathbf{H}_0 \parallel \mathbf{r}$ the field dependence of f extracted from the $M(H_0)$ curves are qualitatively similar to that obtained for $\mathbf{H}_0 \parallel \mathbf{c}$, shown in Fig. 2. Typical field dependence of the ratio of the magnetic moments M_c/M_r , that of sample 1, is presented in Fig. 4. For very low fields it equals $(1-N_r)/(1-N_c) \approx 1.6$ and then it drops to a smaller value and stays essentially constant throughout the entire studied field range including $H_g > H_{c1}^{\text{grains}}$. According to Eq. (8) this ratio is

$$\frac{M_c}{M_r} = \frac{H_0 - B_s^c}{H_0 - B_s^r} \frac{f_c}{f_r} \frac{1 - N_{\text{eff}}^r}{1 - N_{\text{eff}}^c}. \quad (13)$$

For $H_s < H_{c1}^{wl}$, where $B_s = 0$, $f_c = f_r$, and $N_{\text{eff}} \approx N$, and thus the ratio equals $(1-N_r)/(1-N_c)$. For larger fields the independence of this ratio reflects the mutual change of both f_c/f_r and $(1-N_{\text{eff}}^r)/(1-N_{\text{eff}}^c)$. The fact that this ratio does not alter upon crossing H_{c1}^{grains} points to the insignificant contribution of B_s to it in the studied field interval.

C. Results related to samples 7 and 8

Figure 5 shows the shielded fraction of samples 7 and 8, for $\mathbf{H}_0 \parallel \mathbf{c}$ as a function of H_0 , and from a mere glance it is apparent that there is no sharp decrease, which is characteristic for the contribution of the weak links. The shielded fraction is constant up to H_{c1}^{grains} , which is not well defined due to the scattered grains characteristics. The absence of the weak links features in Fig. 5 is readily understood, since both samples were prepared by dispersing fine Y-Ba-Cu-O powder in a polymer, a procedure that destroys most weak links. The values of f in the

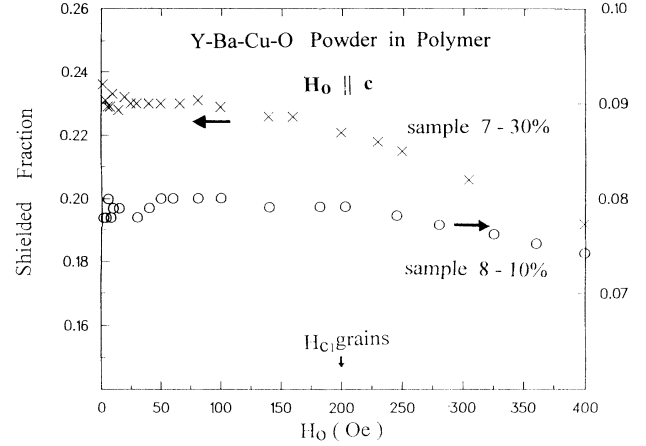


FIG. 5. The applied field dependence ($\mathbf{H}_0 \parallel \mathbf{c}$) of the shielded fraction f of samples 7 and 8 prepared by dispersing fine Y-Ba-Cu-O powder in polymer. Note that f is essentially constant up to H_{c1}^{grains} . The decrease of f at higher fields is less significant than presented in this figure, since the assumption that $B_s = 0$ is not justified at these fields.

low-field limit (0.24 and 0.08 for samples 7 and 8, respectively), allows us to estimate that the relative contribution of nonsuperconducting material to the total volume of the Y-Ba-Cu-O powder is about 20%.

These samples were also measured in the perpendicular direction, yielding the ratio

$$M_c/M_r < (1-N_r)/(1-N_c),$$

nearly field independent throughout the whole studied field interval.

It is instructive to compare the previous results with results obtained on a melt textured sample (packing factor = 80%). This sample, as characterized by SEM, is composed of $100 \times 50 \times 15 \mu\text{m}^3$ (typical size) bricklike grains, nearly perfectly oriented one on top of the other with the thin dimension parallel to the axis of the cylinder. The amount of intergranular material is negligible. Qualitatively speaking the field dependence of f for this sample is similar to that of samples 7 and 8 shown in Fig. 5. The shielded fraction is constant up to H_{c1}^{grains} , with no evidence for existence of weak links of significant volume. The ratio M_c/M_r of this sample is constant up to H_{c1}^{grains} and regularly decreases at higher fields. This is in sharp contrast to the results obtained on the intrinsically isotropic samples (1–8), for which this ratio was nearly field independent, for $H > H_{c2}^{wl}$ (Fig. 4). It is, therefore, that M_c and M_r of the melt-textured sample could not be scaled in a similar manner to that presented in Fig. 1(b). The experimental details related to the melt-textured sample will be published elsewhere.¹⁵

V. CONCLUSIONS

Applying the Clausius-Mossotti approach to the problem of granular ceramic superconductors, we suggest a phenomenological model. According to the model the

effective demagnetizing factors depend on the fraction of shielded volume, which is for itself a field-dependent quantity. We have used this model to evaluate magnetization measurements of granular Y-Ba-Cu-O samples of different packing factors. The model enables us to trace the field dependence of both the shielded fraction and the effective demagnetizing factors. From the field dependence of these values we extract the different contributions to the volume of the sample and the relevant critical fields. For samples with well formed weak link $H_{c1}^{wl} \approx 10$ Oe and $H_{c2}^{wl} \approx 50$ Oe. We found that slow cooling rates lead to a formation of homogeneous weak links and to a combination of some amount of shielded pores to a larger unshielded pore. For intrinsically isotropic samples we

observed nearly field-independent anisotropy ratio of the magnetic moments.

ACKNOWLEDGMENTS

The melt-textured sample was grown at the Crown Center for Superconductivity, Technion, Haifa, Israel, by L. Patlagan and O. David. This research was supported by a grant from the Ministry of Science and Technology, Jerusalem, Israel, by the Klachky Foundation for Superconductivity and by a grant from the U.S.-Israel Binational Science Foundation (BSF), Jerusalem, Israel.

¹D. Chen, J. A. Brug, and R. B. Goldfarb, IEEE Trans. Magn. **27**, 3601 (1991).

²T. T. Taylor, J. Res. Nat. Bur. Stand. **64B**, 199 (1960).

³M. N. Kunchur and S. J. Poon, Phys. Rev. B **43**, 2916 (1991).

⁴S. Senoussi, S. Hajoudj, R. Maury, and A. Fert, Physica C **165**, 364 (1990).

⁵J. Clerk Maxwell, *A Treatise on Electricity and Magnetism*, 3rd ed. (Clarendon, Oxford, 1892), Vol. 2, pp. 66–73 [Reprinted (Dover, New York, 1954)].

⁶U. Yaron, I. Felner, and Y. Yeshurun, Phys. Rev. B **44**, 12 531 (1991); S. Senoussi and C. Aguilon, Europhys. Lett. **12**, 273 (1990).

⁷J. Osborn, Phys. Rev. **67**, 351 (1945).

⁸S. Reich and V. M. Nabutovsky, J. Appl. Phys. **68**, 668 (1990).

⁹M. L. Holdron, R. Navarro, and L. J. Campbell, Europhys. Lett. **16**, 667 (1991).

¹⁰C. J. F. Bottcher, *Theory of Electric Polarization* (Elsevier, Amsterdam, 1973), pp. 168–200.

¹¹D. A. G. Bruggeman, Ann. Phys. (Leipzig) **24**, 636 (1935).

¹²R. Landauer, in *Electrical Transport and Optical Properties of Inhomogeneous Media*, Proceedings of the First Conference on the Electrical Transport and Optical Properties of Inhomogeneous Media, edited by J. C. Garland and D. B. Tanner, AIP Conf. Proc. No. 40 (AIP, New York, 1978).

¹³C. P. Bean, Phys. Rev. Lett. **8**, 250 (1962).

¹⁴Y. B. Kim, Rev. Mod. Phys. **36**, 39 (1964).

¹⁵U. Yaron, Y. Korniyushin, I. Felner, O. David, and L. Patlagan (unpublished).